TOXICOLOGICAL SCIENCES **138(1)**, 175–190 2014
doi:10.1093/toxsci/kft276
Advance Access publication December 12, 2013

Transcriptome Profiling of the Newborn Mouse Lung Response to Acute Ozone Exposure

Kelsa Gabehart,* Kelly A. Correll,* Jing Yang,* Maureen L. Collins,* Joan E. Loader,*,[1], Sonia Leach,† Carl W. White,*,[1] and Azzeddine Dakhama*,[2]

*Department of Pediatrics and
†Department of Medicine, National Jewish Health, Denver, Colorado 80206

[1]Present address: Department of Pediatrics, Children's Hospital, University of Colorado Denver-Anschutz Medical Campus, Aurora, Colorado 80206.
[2]To whom correspondence should be addressed at Department of Pediatrics, National Jewish Health, 1400 Jackson Street, Denver, CO 80206.
Fax: (303) 270-2182. E-mail: dakhamaa@njhealth.org.

Received August 21, 2013; accepted December 3, 2013

Ozone pollution is associated with adverse effects on respiratory health in adults and children but its effects on the neonatal lung remain unknown. This study was carried out to define the effect of acute ozone exposure on the neonatal lung and to profile the transcriptome response. Newborn mice were exposed to ozone or filtered air for 3 h. Total RNA was isolated from lung tissues at 6 and 24 h after exposure and was subjected to microarray gene expression analysis. Compared to filtered air-exposed littermates, ozone-exposed newborn mice developed a small but significant neutrophilic airway response associated with increased CXCL1 and CXCL5 expression in the lung. Transcriptome analysis indicated that 455 genes were down-regulated and 166 genes were up-regulated by at least 1.5-fold at 6 h post-ozone exposure (*t*-test, $p < .05$). At 24 h, 543 genes were down-regulated and 323 genes were up-regulated in the lungs of ozone-exposed, compared to filtered air-exposed, newborn mice (*t*-test, $p < .05$). After controlling for false discovery rate, 50 genes were identified as significantly down-regulated and only a few (RORC, GRP, VREB3, and CYP2B6) were up-regulated at 24 h post-ozone exposure ($q < .05$). Gene ontology enrichment analysis revealed that cell cycle-associated functions including cell division/proliferation were the most impacted pathways, which were negatively regulated by ozone exposure, an adverse effect that was associated with reduced bromo-deoxyuridine incorporation. These results demonstrate that acute ozone exposure alters cell proliferation in the developing neonatal lung through a global suppression of cell cycle function.

Key Words: **ozone; neonatal lung; gene expression.**

Ozone (O_3) is a common urban air pollutant generated through chemical reactions of nitrogen oxides and volatile organic compounds in the presence of heat and UV sunlight. O_3 is a highly reactive and insoluble gas that can be inhaled from polluted air environment and causes many adverse effects on respiratory health, including alterations in the structure of the airway epithelium, increased sensitivity to inhaled allergens, increased airway inflammation, and altered lung function (Mar and Koenig, 2009; Romieu *et al.*, 2002; Strickland *et al.*, 2010).

Young children are particularly vulnerable to developing adverse respiratory health effects from O_3 exposure due to higher ventilation rates, potentially leading to higher doses of inhaled O_3 during exposure. Infants are also highly susceptible and at risk of developing respiratory symptoms even with low levels of O_3 exposure, particularly if their mothers have asthma (Triche *et al.*, 2006). In addition, their lungs are still incompletely developed, with up to 80% of alveolarization occurring after birth (Dietert *et al.*, 2000; Pinkerton and Joad, 2000), and damage to the lung during this window of development may potentially have long-term negative impacts on their respiratory health. Differential sensitivity of developing lungs to environmental pollutants may also be explained by differences in the maturation of inflammatory and defense mechanisms, as indicated by experimental data from animal studies (Gabehart *et al.*, 2011, Holladay and Smialowicz, 2000; Johnston et al., 2000a, 2004, 2006; Vancza *et al.*, 2009).

In the pediatric population, high ambient O_3 levels are widely associated with an increase in asthma-related emergency department visits (Babin *et al.*, 2007; Strickland *et al.*, 2011; White *et al.*, 1994). Even mildly elevated O_3 levels over longer periods can increase asthma exacerbation and attacks (Akinbami *et al.*, 2010). Exposure to air pollution, especially during the postnatal lung development period can damage the airways which may subsequently lead to a deficit in lung function (Finkelstein and Johnston, 2004; Pinkerton and Joad, 2000; Plopper and Fanucchi, 2000). Epidemiological studies have demonstrated a correlation between high ambient O_3 levels and lower lung function in young adults (Tager *et al.*, 2005), but there remain conflicting results regarding long-term effects of O_3 exposure. Intermittent, cyclical exposure to O_3 was shown to alter the development of

© The Author 2013. Published by Oxford University Press on behalf of the Society of Toxicology.
All rights reserved. For permissions, please email: journals.permissions@oup.com.

distal airways in infant rhesus monkeys (Fanucchi *et al.*, 2006). Nonetheless, our understanding of the effects of O_3 on the developing neonatal lung remains incomplete. This study was carried out to characterize the response of the newborn lung to acute O_3 exposure and to profile the transcriptome response using whole-genome expression analysis. Acute O_3 exposure induced a low-grade neutrophilic airway inflammation with limited tissue-damage in the neonatal mouse lung. Analysis of the lung transcriptome demonstrates that the most predominant impact of O_3 on the developing neonatal lung was a global suppression of functional genes involved in cell cycle, cell division, cellular assembly and organization, an adverse effect that was associated with reduced cell proliferation in the lung.

MATERIALS AND METHODS

This study was carried out in accordance with the recommendations of the National Institutes of Health Guide for the Care and Use of Laboratory Animals. All experiments were carried out under a protocol approved by the Institutional Animal Care and Use Committee at National Jewish Health. All surgery was performed under terminal anesthesia with pentobarbital.

The microarray data from this study have been submitted to Gene Omnibus. Submission link: (http://www.ncbi.nlm.nih.gov/geo/query/acc.cgi?token=vnanfmqkuwaqonc&acc=GSE45166).

General experimental design. Three-day old BALB/c mice were exposed with their dams to 1000 ppb O_3 for 3 h. Because the lungs are growing rapidly during this early postnatal phase, littermates were used as controls for filtered air (FA) exposure to ensure similar postnatal development age for both groups. Thus, while half the litters were exposed with their dams to O_3, the other half (age-matched controls) were fostered by other dams and exposed together to FA. Exposure of pups with nursing dams was designed to avoid potential effect of stress that could be caused by mother/infant separation during the exposure. Immediately after exposure, the FA pups were returned to their original dams to maintain the same nursing habits and to control for potential confounding effects of pups feeding from ozone-exposed dams. Samplings were carried out immediately after euthanasia, at 6 and 24 h following completion of exposure. These time points were selected from preliminary experiments with adult (6-week old) BALB/c mice showing peak responses for neutrophilic influx at 6 h and maximum albumin leakage at 24 h following completion of 3 h exposure to 1000 ppb (data not shown).

After euthanasia, the neonatal lungs were lavaged and processed for histology. Inflammation was examined by counting the number of inflammatory cells recovered in the bronchoalveolar lavage (BAL) fluid. Pulmonary injury was assessed by measuring the concentration of albumin in the recovered BAL fluids and by histological examination of airway tissue. Neutrophilic chemokine expression and antioxidant gene response were assessed by real-time quantitative polymerase chain reaction (rt-qPCR). Whole lungs without lavage were used for RNA isolation and transcriptome analysis. Changes in gene expression were confirmed by rt-qPCR for selected genes. In separate experiments, bromodeoxyuridine (BrdU) was injected to the animals 3 h before euthanasia to assess the effect of O_3 on cell proliferation *in vivo*, confirming that the global suppression of cell cycle genes detected by transcriptome analysis translated into a decrease in lung cell proliferation.

Animals. Adult (6–8 weeks old) BALB/c mice were obtained from The National Cancer Institute Mouse Repository (Frederick, MD). BALB/c mice were shown to be one of the most sensitive strains to O_3 (Vancza *et al.*, 2009). Mice were bred and maintained under pathogen-free conditions at the Biological Resource Center of National Jewish Health. The study was under a protocol approved by the Institutional Animal Care and Use Committee at National Jewish Health.

Exposures. Three-day old newborn BALB/c mice were exposed to 1000 ppb O_3 or FA for 3 h in stainless steel wire cages. O_3 exposures were performed as previously described (Park *et al.*, 2004). Cages were set inside a 240-l laminar flow inhalation chamber. HEPA-filtered room air was passed through the chamber at 100 l per min. O_3 was generated by passing compressed medical-grade oxygen through an electrical discharge ozone generator (Sander Ozonizer, Model 25; Erwin Sander Elektroapparatebau GmbH, Uetze-Eltze, Germany). The O_3-air mixture was metered into the inlet air stream with mass flow controllers (Model #1359C; MKS Instruments, Inc., Andover, MA). Ozone concentrations were continuously monitored within the chamber with a photometric ozone analyzer (Model 400A; Advanced Pollution Instrumentation, Inc., San Diego, CA) and were recorded on a strip-chart recorder. Calibration of the ozone analyzer was performed by the Colorado Department of Public Health and Environment (Denver, CO). Chamber temperature was maintained at 20–25°C.

BAL, cell counting and measurement of albumin levels. BAL was performed at 6 and 24 h after completion of exposure to O_3 or FA. Mice were euthanized by intraperitoneal injection of pentobarbital (Nembutal, 100 mg/kg body weight), the trachea was cannulated with a 25G blunt-end needle, and the lungs were lavaged via the cannula with 150 µl of phosphate-buffered saline (PBS). The recovered BAL fluids were centrifuged at 485 × g for 5 min at 4°C. Supernatants were collected and stored at −80°C until needed for subsequent analyses. Cells in the pellet were suspended in 100 µl PBS and total numbers were determined by counting on ABC Vet hematology analyzer (Block Scientific, Bohemia, NY). Differential cell counts were determined by standard hematological procedures, counting different cell types on cytospin preparations of BAL cells stained with Leukostat (Fisher Diagnostics, Pittsburgh, PA). Albumin levels in the BAL fluids were quantified used a mouse-specific ELISA (Bethyl Laborotories, Montgomery, TX).

Lung tissue processing for histology. For histology, the lungs were inflated in situ with 4% paraformaldehyde in phosphate-buffered saline (PBS) administered through the tracheal cannula at a 20-cm static fluid pressure. Briefly, the trachea was cut open in the most proximal region close to the pharynx. The cannula, consisting of 25G blunt needle, was inserted into the trachea just enough (about 2–3 mm deep) to secure it in place with a 4-0 silk suture (Kent scientific Corp., Torrington, CT). The fixative was placed in a 50-ml syringe, with a 30-cm long flexible tube (Tygon tubing, 2.4-mm internal diameter, Fisher Scientific) connecting the syringe to a 2-way stopcock. The fixative was allowed to flow through the tubing to remove air, after which the stopcock was closed and connected to the cannula. The syringe was then elevated so that the top level of the fixative inside the syringe is at a height of 20-cm above the level of the mouse trachea. Finally, the stopcock was opened allowing the fixative to fill the lung by static gravity. The instillation was maintained for 5 min after which, the stopcock was closed, and the trachea was tied up and cut below the insertion position of the cannula. The lungs were removed and immersed in the same fixative for 24-h fixation at 4°C, followed by dehydration in graded ethanols, clearing in xylene and embedding in paraffin. Five-micron tissue sections were cut from the paraffin blocs, deparaffinized, rehydrated, and stained with hematoxylin and eosin.

Tissue processing for electron microscopy. For electron microscopy, the trachea was dissected and fixed for 24 h at 4°C with glutaraldehyde (1.5% in 0.1 M cacodylate buffer, pH 7.2), washed in cacodylate buffer and post-fixed for 1 h at room temperature in osmium tetroxide (1% in cacodylate buffer). The fixed tissues were then dehydrated, infiltrated with araldite and embedded in the same resin. Ultrathin tissue sections were cut on a LKB Ultramicrotome using a diamond knife. The sections were stained with uranyl acetate and contrasted with lead citrate. Sections were examined under JEOL 1200 transmission electron microscope.

Lung tissue harvest and mRNA extraction. Mice exposed exclusively for microarray gene expression analyses were not subjected to bronchoalveolar lavage to avoid eliminating resident alveolar cells including alveolar macrophages and potentially detached epithelial cells, which may also express genes of interest. Mice were euthanized by intraperitoneal injection of pentobarbital

(Nembutal, 150 mg/kg body weight). Blood was drained by severing the aorta and whole lungs were collected, placed in RNAlater (Qiagen), and stored at 4°C until extraction. Total RNA was extracted using TRIzol RNA isolation reagent (Invitrogen, Carlsbad, CA) and cleaned up using miRCURY RNA Isolation Kit (Exiqon, Woburn, MA) following the manufacturers' instructions. RNA concentration and purity were examined by spectrophotometry with a NanoDrop ND-100 Spectrophotometer (NanoDrop, Willington, DE). RNA quality was assessed using Agilent 2100 Bioanalyzer (Agilent Technologies, Santa Clara, CA). RNA integrity values ranged between 8.6 and 9.1, and 28S/18S ratios ranged between 1.0 and 1.4.

Gene expression microarrays. Four individual lungs were randomly selected from each group (O_3, FA) and time point (6 h, 24 h) for use in gene expression analysis. Processing of the microrrays and quality control tests were performed by the Center for Genes, Environment and Health, at National Jewish Health (Denver, CO). Microarray analysis was performed using Whole Mouse Genome Gene Expression 4X44K Microarrays (G2519F-014868, Agilent Technologies). Each array contains probes for 39,430 Entrez Gene RNAs. Labeling was performed using the Quick-Amp Labeling Kit (5190-0442, Agilent Technologies). For all samples, first strand cDNA was transcribed from 600 to 1000 ng of total RNA using a T7-Oligo(dT) promoter primer. Subsequent synthesis of cRNA generated between 7.0 and 22.0 ng of Cy-3 labeled cRNA. Unincorporated nucleotides were removed from the labeled cRNA using RNeasy spin columns (Qiagen). Quality control parameters (cRNA yield and specific activity of labeled RNA) were assessed using the NanoDrop 1000 (Thermo Scientific) as recommended by Agilent Technologies. Labeled cRNA was fragmented and 1.65 micrograms from each sample were hybridized to each array using the Hybridization Kit (Agilent Technologies). Hybridization was performed at 65°C for 17 h with constant rotation. Arrays were washed in a two-step process using buffers from Agilent Technologies. Arrays were scanned in a G2505B scanner (Agilent Technologies) and images were processed using Agilent Feature Extraction software. All arrays passed QC as assessed by the manufacturer's established metrics.

Gene expression analysis. Analysis of datasets was performed using Partek Genomics Suite software (Partek, Inc., St Louis, MO). To minimize non-biological variability across and within array samples the raw data were $\log_2$ transformed and quantile normalized. Student's *t*-test *p*-values were determined and multiple comparison error was corrected for using the Benjamini and Hochberg step-up procedure for multiple comparisons to determine significance at a false discovery rate of 5% ($q < 0.05$) (Benjamini and Hochberg, 1995).

Gene ontology enrichment analysis. Functional analysis was performed by gene ontology (GO) enrichment using Partek Genomics Suite software. Molecules from the dataset were annotated with GO terms and statistical analysis of enriched biological function groups was determined with Fisher's exact test.

Pathway analysis. Gene expression pathways were analyzed and mapped using the Ingenuity Knowledge Base (Ingenuity Systems, www.ingenuity.com). The network molecules associated with biological functions in the Ingenuity Knowledge Base were considered for analysis. Functional analysis identified most significant biological functions within the network. Right-tailed Fisher's exact test was used to determine the probability that each biological function assigned to a network is due to chance alone.

Real-time qPCR. To confirm and further explore differential mRNA expression in the postnatal lung exposed to O_3, rt-qPCR was performed for selected genes. RNA was converted to cDNA with M-MLV Reverse Transcriptase (Promega, Madison, WI). Taqman Gene Expression Assays for various genes and Taqman Universal PCR Master Mix (Life Technologies, Grand Island, NY) were used to perform rt-qPCR on an ABI Prism Model 7000 Real Time PCR machine.

Bromodeoxyuridine incorporation and analysis of cell proliferation. To assess cell proliferation in the lung, mice were injected intraperitoneally with the thymidine analog bromodeoxyuridine (BrdU, 100 mg/kg in 10 µl PBS/g of body weight) 3 h prior to euthanasia. The lungs were inflated at 20 cm pressure with 4% paraformaldehyde through a tracheal cannula, fixed at 4°C for 24 h, and rinsed with PBS. The left lobe was rotated to a 90° angle relative to the right lobes, and the entire lung was embedded in 4% agarose with random positioning as described in Knust *et al.* (2009). The agarose-embedded lungs were then serially cut into 1.2-mm thick longitudinal slices. The slices were dehydrated, cleared and embedded in paraffin. Serial tissue sections were cut on the microtome at 5-µm thickness, deparaffinized and rehydrated. Bromodeoxyuridine was detected in tissue by immunohistochemistry as follows. After quenching endogenous peroxidase with 3% H_2O_2 for 10 min, the sections were incubated in 2 N HCl for 30 min at 37°C to denature DNA, followed by incubation with pepsin (Scytek Laboratories, Logan, UT) for 10 min at 37°C to retrieve antigen and washed with 50 mM Tris-buffered saline, pH 7.6 (TBS). After blocking non-specific background by 15-min incubation with 5% normal goat serum, the sections were incubated for 2 h at 37°C with a mouse monoclonal anti-BrdU antibody (DAKO, Carpinteria, CA), washed with TBS and further incubated for 30 min at room temperature with ImmPRESS Anti-Mouse Ig (peroxidase) Polymer Detection kit (Vector Laboratories, Burlingame, CA), followed by washing in TBS and development with DAB substrate. Stained serial tissue sections were scanned at 20× magnification on Aperio ScanScope XT slide scanner (Aperio, Vista, CA) and digital images were transferred to the computer for quantitative analysis of proliferating cells by unbiased stereology using Stereo Investigator Pulmonary Edition software (MBF Bioscience, Williston VT). Proliferating cells were identified as cells with BrdU-positive nuclei. Data are presented as numbers of BrdU-positive cells per volume of tissue analyzed.

Statistical analysis. Microarray data were analyzed using Partek Genomics Suite software. Statistical differences in gene expression between ozone and filtered air groups were determined by Student's *t*-test ($p < .05$). The Benjamini–Hochberg procedure was further applied to limit false discovery rate to 5% ($q \leq .05$). For gene ontology and pathway analyses, statistical significance was determined with Fisher's exact test ($p \leq .05$). Data from BAL cell counts, ELISA, and RT-qPCR were analyzed using GrahPad Prism version 5.0 for Mac OS X (GraphPad Software, San Diego, CA). Difference between the groups was determined by Student's *t*-test or Mann–Whitney *U* test. For more than two groups, one-way ANOVA was used followed by Tukey's multiple comparisons to determine statistical difference. Statistical difference was defined by a *p* value <.05.

RESULTS

Effect of O_3 Exposure on the Newborn Mouse Lung

Acute exposure of newborn mice to O_3 for 3 h resulted in the development of mild but significant airway neutrophilia that peaked at 6 h after exposure (Fig. 1A). No significant change was observed in macrophage or lymphocyte numbers (Figs. 1B and 1C), and albumin levels in the recovered BAL fluid were not significantly altered after O_3 exposure (Fig. 1D). Associated with the influx of neutrophils, there was a significant increase in mRNA expression for the neutrophilic chemokines CXCL1 and CXCL5 in the lung of O_3-exposed mice (Figs. 1E and 1F), whereas CXCL2 mRNA expression was not altered (data not shown). O_3 exposure also induced an antioxidant response in the newborn lung, as indicated by a significant increase in mRNA expression for metallothionein-1 (MT-1) and heme oxygenase-1 (Hmox-1) (Figs. 1G and 1H).

Histological examination of paraffin-embedded lung tissue did not reveal any significant damage or loss of epithelial cells, as determined by lack of epithelial detachment or denudation, in

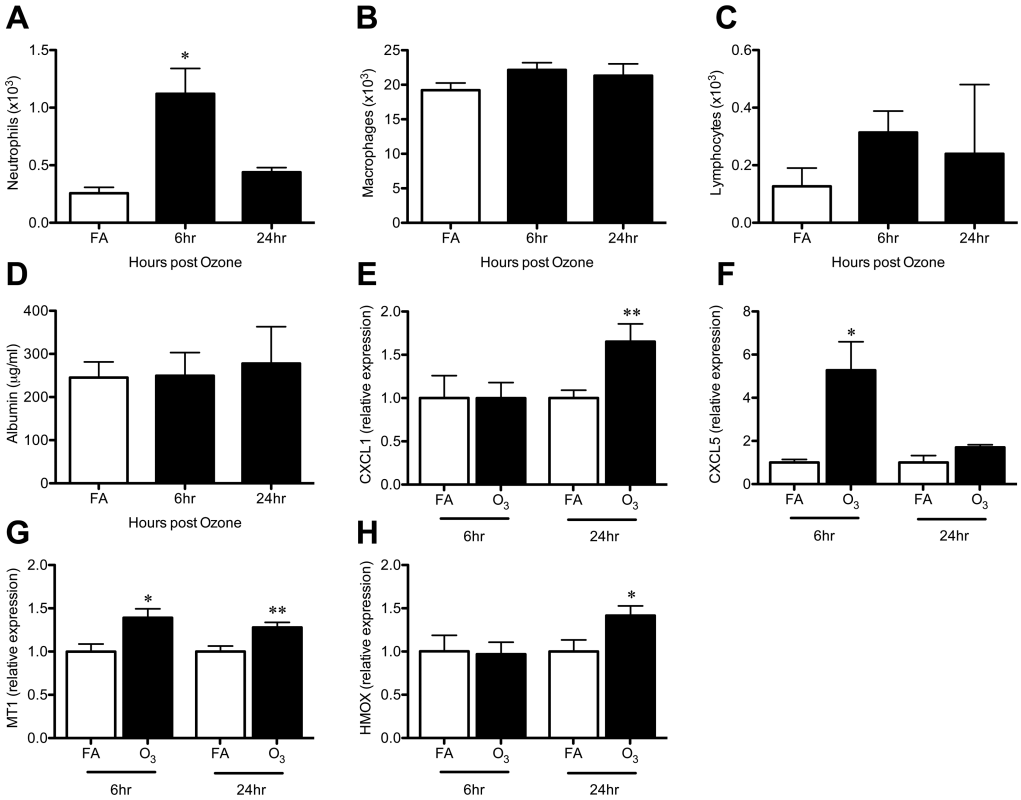

FIG. 1. Effect of acute O_3 exposure on neonatal lung. Newborn mice were exposed for 3 h to FA or O_3. Analyses were carried out at 6 and 24 h after completion of exposure. Numbers of neutrophils (A), macrophages (B) and lymphocytes (C), and albumin levels (D) were determined in the BAL fluid. Expression of neutrophilic chemokines, CXCL-1 (E) and CXCL-5 (F), and antioxidant response genes, MT-1 (G) and Hmox-1 (H), were assessed in lung tissue by RT-qPCR.

the neonatal lungs after acute O_3 exposure (Fig. 2B). However, when tracheal tissue was examined by electron microscopy (Figs. 2C–E), significant alterations in the epithelial structure were detected in O_3-exposed newborn mice. Most notably, the intercellular space between epithelial cells was clearly enlarged especially in the baso-lateral side (Fig. 2D, arrows), and a complete gap could be observed between 2 adjacent epithelial cells in the trachea of O_3-exposed mice (Fig. 2E, asterisk).

Global Gene Expression Patterns in the Newborn Lung After O_3 Exposure

In the postnatal period, the lung develops rapidly and changes in transcriptome are expected to occur in a short window of time. Accordingly, we carefully designed this study using age-matching littermates as controls for FA exposure to specifically identify the changes induced by O_3, distinguishing them from those changes that occur naturally as result of normal lung development. When the effect of O_3 exposure was analyzed, a 1.5-fold change in gene expression in the O_3 group relative to the FA group was set as a cutoff value for identification of differentially expressed genes with a p-value of 0.05 (Student's t-test). In total, 621 genes and 866 genes were differentially expressed at 6 and 24 h, respectively, in the lungs of O_3-exposed newborn mice compared with FA-exposed newborn mice. As illustrated in Venn diagrams, the total number of genes down-regulated by O_3 was 455 at 6 h and 543 at 24 h after exposure (Fig 3A). Among these, 77 genes were down-regulated at both time points. In parallel, the total number of genes up-regulated by O_3 was 166 at 6 h and 323 at 24 h after exposure; including 7 genes that were up-regulated at both time points (Fig. 3B).

Top List of Differentially Expressed Genes

Based on Student's t-test analysis, a total of 621 genes that were differentially expressed at 6 h post exposure with a p-value of less than .05 in the O_3 group. However, after controlling for false discovery rate (FDR) using the Benjamini–Hochberg procedure for multiple comparisons, none of these genes qualified as significantly altered in expression based on a conservative FDR set at 5% ($q < .05$). At best, only 40 genes were displayed with a less conservative FDR cutoff value of 15% (Table 1). Among these genes, 11 were up-regulated and 29 were down-regulated at 6 h post O_3 exposure ($q < .15$). Nevertheless, hierarchical clustering analysis performed with this probe set clearly distinguished O_3-exposed from FA-exposed mice (Fig. 4A).

At 24 h following O_3 exposure, 866 genes were differentially expressed based on Student's t-test analysis ($p < .05$). Using the Benjamini–Hochberg procedure to control for false discovery rate, a total of 55 genes were identified as significantly altered in expression by at least 1.5-fold with a FDR set

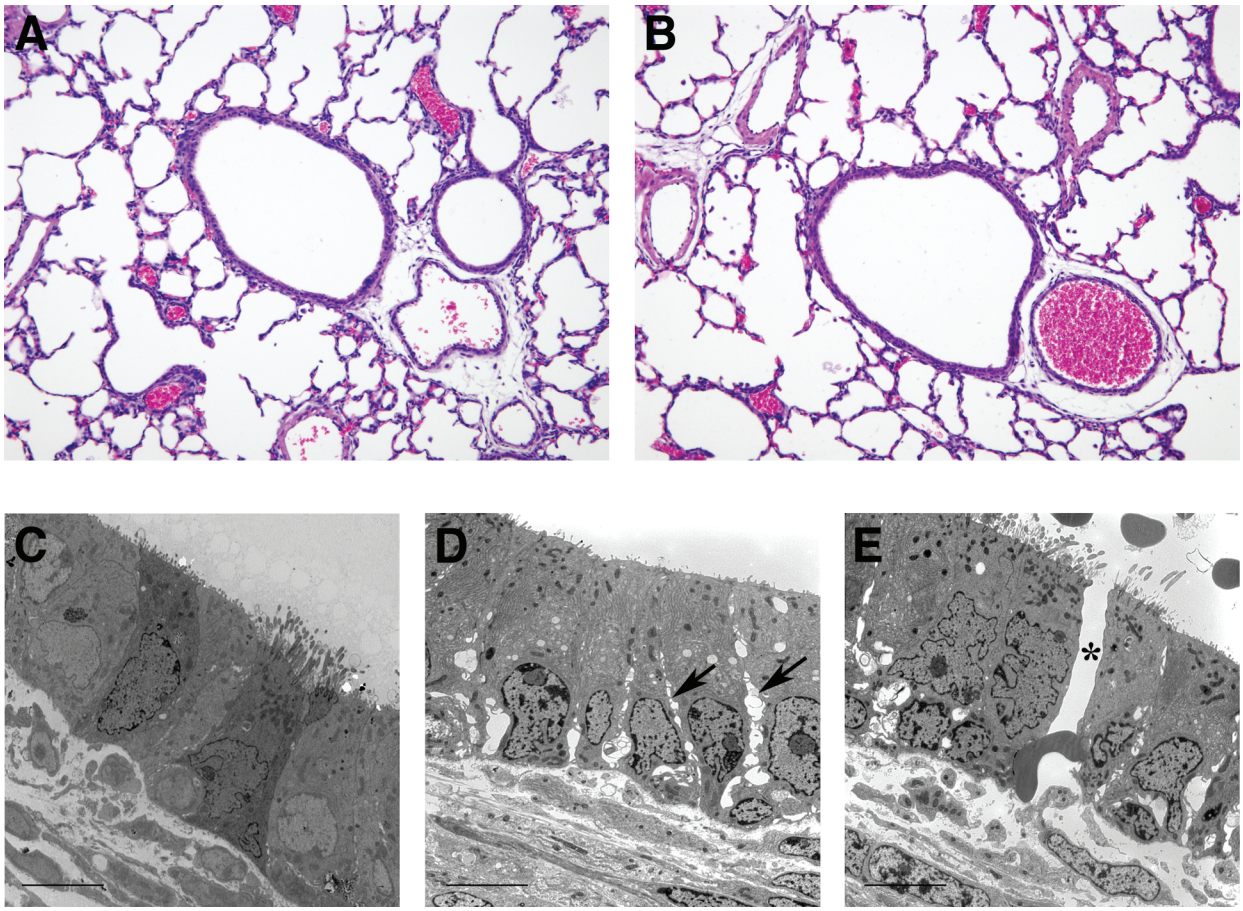

FIG. 2. Histological appearance of newborn airway tissue after acute exposure to O_3 and FA. Newborn lungs were examined 6 h after exposure to FA or O_3. A and B, Paraffin-embedded lung tissue sections from newborn mice exposed to FA (A) or O_3 (B) were stained with hematoxylin and eosin. C and E, Electron microscopy photomicrographs showing the appearance of tracheal epithelium after acute exposure to FA (C) or O_3 (D and E). Note the enlarged intercellular space (D, Arrows) and the open gap between adjacent epithelial cells (E, Asterisk) produced in the epithelium after O_3 exposure.

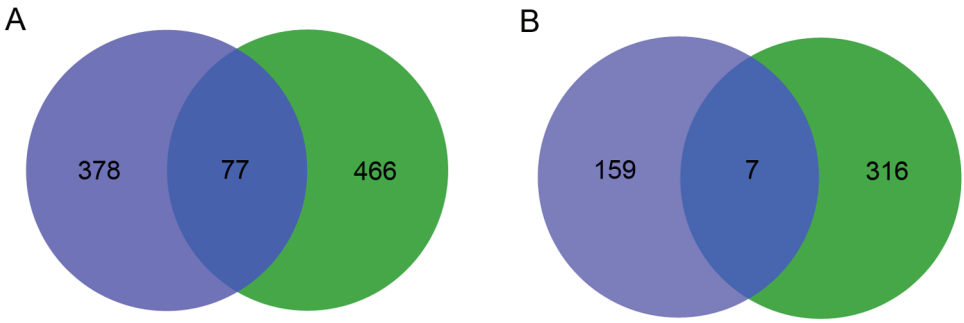

FIG. 3. Number of genes altered in the newborn lung after O_3 exposure. Venn diagrams showing numbers of genes differentially expressed in the neonatal lung at 6 h (left circle), 24 h (right circle), or at both time points (intersection) following O_3 exposure. A, Genes down-regulated in expression by at least 1.5-fold relative to FA controls (*t*-test, $p < .05$). B, Genes up-regulated in expression by at least 1.5-fold relative to FA controls (*t*-test, $p < .05$).

at 5% ($q < .05$). Of these genes, 50 were down-regulated and only 5 were up-regulated (Table 2). Hierarchical clustering analysis performed with this probe set revealed a clear pattern of expression distinguishing O_3-exposed from FA-exposed mice (Fig. 4B).

Gene Functional Enrichment Analysis

Functional groups enriched 24 h after O_3 exposures were identified by Gene Ontology enrichment analysis using Partek Genomic Suite software (Table 3). All of the genes listed in Table 2, which were significantly changed in expression by at

TABLE 1
Top List of Genes Differentially Expressed in Newborn Lung at 6 h After O_3 Exposure[a]

Agilent Probeset ID	Gene Name	Fold Change	*p*-Value	FDR
A_51_P318262	HAO1	2.68	1.40E-04	0.129
A_51_P333929	COL25A1	2.00	5.20E-04	0.147
A_51_P271200	Slco1a5	1.98	2.30E-04	0.137
A_52_P249965	XDH	1.84	7.50E-05	0.129
A_52_P448045	TSPAN18	1.68	1.10E-04	0.129
A_51_P189361	OSGIN1	1.68	5.30E-04	0.147
A_51_P486810	GPX2	1.60	2.60E-04	0.14
A_51_P451574	Acot1	1.56	2.20E-04	0.137
A_51_P507359	WBSCR27	1.52	4.00E-04	0.147
A_52_P13109	ALDH2	1.51	4.90E-04	0.147
A_51_P351872	SLC6A9	1.50	5.50E-04	0.148
A_52_P27918	ATAD5	−1.50	9.80E-05	0.129
A_51_P202857	Cdca7	−1.51	2.20E-05	0.114
A_51_P116289	FAM54A	−1.51	4.60E-04	0.147
A_51_P107321	OXCT1	−1.52	2.90E-04	0.141
A_51_P297968	PDIA6	−1.53	2.20E-05	0.114
A_51_P424810	NCAPG2	−1.54	2.70E-04	0.14
A_51_P213359	HAS2	−1.54	5.30E-04	0.147
A_51_P475523	BRCA1	−1.57	2.80E-04	0.141
A_51_P253904	NME1	−1.61	3.30E-04	0.147
A_51_P396351	PCNA	−1.63	5.00E-05	0.129
A_52_P251703	VCAN	−1.64	2.00E-04	0.135
A_51_P466673	SRSF7	−1.66	1.30E-04	0.129
A_51_P419286	BATF3	−1.69	1.30E-04	0.129
A_51_P492830	CENPH	−1.71	4.10E-04	0.147
A_51_P397200	C7orf10	−1.71	3.90E-04	0.147
A_52_P681930	SLC22A6	−1.77	8.60E-05	0.129
A_52_P329197	DHFR	−1.79	3.40E-04	0.147
A_52_P381303	GINS2	−1.80	2.10E-04	0.137
A_52_P655890	WDHD1	−1.82	1.60E-04	0.131
A_51_P269687	POLE2	−1.84	4.50E-04	0.147
A_52_P148553	FIGNL1	−1.87	3.20E-04	0.147
A_51_P401451	CDC45	−1.95	1.40E-04	0.129
A_51_P347240	LRR1	−1.97	2.00E-04	0.135
A_51_P337083	GINS1	−1.99	3.90E-04	0.147
A_52_P285722	HELLS	−2.33	5.20E-04	0.147
A_52_P655239	RHOT1	−2.51	1.80E-04	0.134
A_52_P33097	PRR11	−2.62	2.70E-04	0.14
A_52_P203316	KCNF1	−2.98	1.30E-04	0.129
A_52_P271671	CNTN4	−3.51	5.60E-05	0.129

[a]Included are all genes altered by at least 1.5-fold in expression and detected with a FDR of less than 0.15.

least 1.5-fold ($q < .05$) at 24 h post-O_3 exposure, were used for this analysis. Several of the functional genes identified were involved in cell cycle and cell division. More detailed description of these genes and their related function is presented in Supplementary Table E1. The highest enrichment score was obtained for the Cell Cycle functional group and involved 18 genes, all down-regulated after O_3 exposure. Other differentially expressed genes associated with the functional groups cell division, cell cycle process, and cell proliferation, were also all down-regulated (Table 3).

Gene Expression Pathway Analysis

Network analysis of genes significantly altered in expression by at least 1.5-fold ($q < .05$) at 24 h post-O_3 exposure identified two major networks with 24 and 15 identified focus molecules and corresponding enrichment scores of 55 and 30 (Table 4, Figs. 5 and 6). Both networks involve Cell Cycle, Cellular Assembly and Organization, DNA Replication, Recombination, and Repair. All these focus genes were down-regulated including the prototypic marker of cell proliferation MKI67, indicating a general suppression of cell proliferation in the newborn lung after acute O_3 exposure.

Figure 7 illustrates the results of rt-qPCR validating the differential expression of selected genes identified by microarray analysis. The results confirmed the down-regulation of mRNA expression seen on the microarrays for MKI67, CDK1, and BRCA, at 24 h post-O_3 exposure. These results also demonstrated that CDK1 and BRCA were significantly

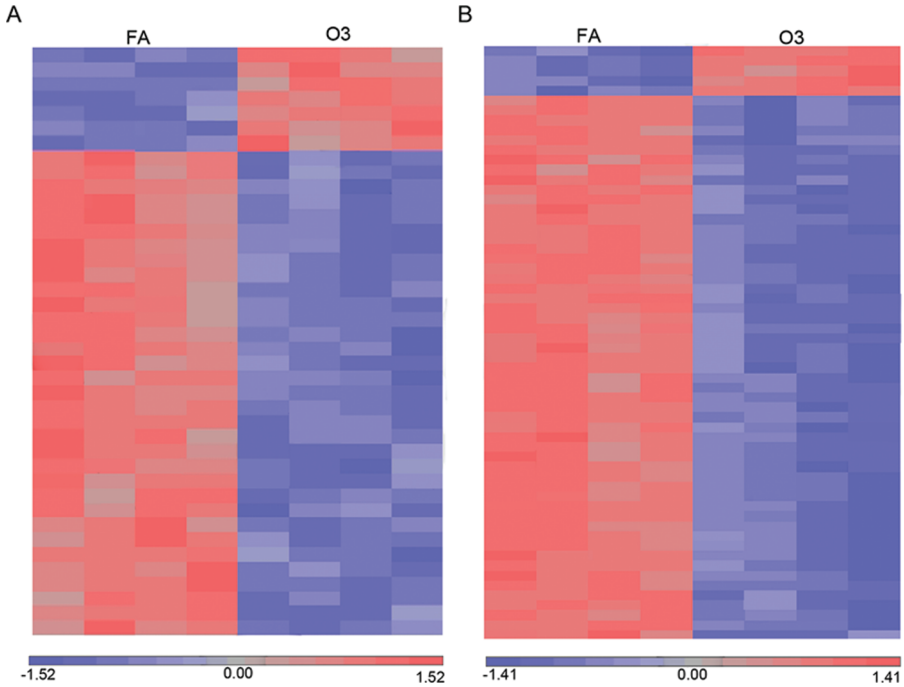

FIG. 4. Hierarchical clustering of genes differentially expressed after O_3 exposure. Heat maps of genes significantly altered in expression by at least 1.5-fold after 6 h (A) and 24 h (B) post-O_3 exposure. FDR cutoff was 0.15 for 6 h (A) and 0.05 for 24 h (B).

down-regulated at 6 h post-O_3 exposure, confirming the trend of decreased expression for these genes on the microarrays, at this early time point. In addition, the results of rt-qPCR also confirmed the increased mRNA expression of RORC and GRP detected after O_3 exposure on the microarrays.

Effect of O_3 Exposure on Cell Proliferation in the Neonatal Lung

To determine if the suppression of cell cycle function-associated genes detected by microarray analysis impacted cell proliferation in the lung of O_3-exposed neonatal mice, we performed in vivo labeling of proliferating cells with the thymidine analogue bromo-deoxyuridine (BrdU). The results were analyzed using quantitative stereology. Proliferating cells were identified by immunohistochemistry as cells positively labeled with BrdU, which incorporated into DNA during synthesis (S-phase) and localized to the nucleus (Figs. 8A and 8B). Quantitative analysis of BrdU-labeled cells revealed that cell proliferation was indeed reduced following acute O_3 exposure in the neonatal lung (Fig. 8C). These findings further demonstrate that the O_3-mediated suppression of cell cycle resulted in reduced cell proliferation in the developing neonatal lung.

DISCUSSION

The overall objective of this study was to define the effects of acute O_3 exposure on the developing neonatal mouse lung at the transcriptome level. To the best of our knowledge, this is the first study to profile the transcriptome response of the newborn lung to O_3 exposure using genome-wide gene expression microarray analysis. The results identified novel genes and molecular pathways never associated before with O_3 exposure. This study was carefully designed with age-matched littermate controls for FA-exposure to identify the changes that are due to O_3 exposure among those naturally occurring during normal development. This is important because the lung is developing rapidly during the neonatal period, and significant changes in lung transcriptome can occur within a short window of time as result of normal development irrespective of O_3 exposure. Thus, independent of these development-related changes, O_3 altered the expression of several genes in the neonatal lung. Of the entire mouse genome analyzed, 621 genes were significantly altered (166 up- and 455 down-regulated) by 6 h and 866 genes were altered (323 up- and 543 down-regulated) by 24 h in the neonatal lung following acute O_3 exposure, when compared with filtered air exposure (Student's t test, $p < .05$). However, using the Benjamini–Hochberg step-wise procedure for multiple comparisons (Benjamini and Hochberg, 1995), a more stringent statistical analysis that controls for false discovery rate, 55 genes were definitely identified as significantly altered at 24 h after acute O_3 exposure (FDR, $q < .05$).

Previous studies that examined the effect of O_3 exposure on gene expression in the lung of adult animals indicate that injury-associated inflammation and tissue repair processes were the most predominant pathways altered by O_3 in fully developed lungs (Gohil *et al.*, 2003; Hicks *et al.*, 2010;

TABLE 2
Top List of Genes Differentially Expressed in Newborn Lung at 24 h After O_3 Exposure[a]

Agilent Probeset ID	Gene Name	Fold Change	*p*-Value	FDR
A_52_P795929	AK081614	2.16	1.10E-04	0.048
A_52_P433847	VPREB3	1.92	5.40E-05	0.043
A_51_P282930	RORC	1.86	8.70E-06	0.022
A_51_P356055	GRP	1.78	2.70E-05	0.035
A_51_P182362	CYP2B6	1.70	7.60E-05	0.044
A_51_P500718	DCK	−1.53	6.90E-05	0.043
A_51_P407606	TMEM48	−1.53	2.60E-05	0.034
A_52_P796682	CCNE1	−1.54	1.50E-05	0.027
A_52_P252737	CHADL	−1.54	6.40E-05	0.043
A_51_P508775	MMP17	−1.56	2.30E-05	0.033
A_52_P247927	2810442I21Rik	−1.58	7.10E-06	0.019
A_51_P108767	RAD54L	−1.59	5.40E-07	0.007
A_52_P363039	NCAPH	−1.61	3.30E-05	0.035
A_52_P184149	MTHFD2	−1.63	4.60E-05	0.041
A_52_P314705	UHRF1	−1.64	5.40E-05	0.043
A_51_P401451	CDC45	−1.65	6.00E-05	0.043
A_52_P364299	MMS22L	−1.67	1.10E-04	0.048
A_51_P314907	DBF4	−1.67	8.20E-05	0.044
A_51_P459100	STIL	−1.72	4.80E-05	0.042
A_52_P304947	CENPN	−1.73	1.90E-06	0.018
A_51_P328333	CCNF	−1.75	6.60E-05	0.043
A_52_P255034	PARPBP	−1.78	1.00E-04	0.047
A_52_P4666	CENPK	−1.80	2.30E-05	0.033
A_51_P441843	FANCI	−1.80	1.00E-05	0.024
A_51_P303749	DEPDC1B	−1.80	1.30E-04	0.049
A_51_P110689	RRM2	−1.80	4.20E-05	0.04
A_52_P220370	ANKLE1	−1.82	1.10E-04	0.048
A_51_P475523	BRCA1	−1.82	4.90E-06	0.019
A_51_P318123	AK084660	−1.82	5.50E-06	0.019
A_51_P358633	MELK	−1.87	1.20E-04	0.048
A_51_P253808	MKI67	−1.88	8.10E-05	0.044
A_52_P399584	CKAP2L	−1.89	3.30E-05	0.035
A_52_P211223	CDCA2	−1.89	7.00E-05	0.043
A_52_P139399	NCAPD2	−1.89	1.60E-05	0.029
A_51_P195034	ESCO2	−1.92	1.20E-04	0.048
A_52_P75348	CCDC99	−1.93	1.00E-04	0.047
A_52_P633714	TROAP	−1.95	3.30E-05	0.035
A_51_P254805	KIF4A	−1.95	1.90E-05	0.027
A_51_P220222	TACC3	−1.97	5.50E-05	0.043
A_52_P584374	KIAA1524	−1.98	6.10E-06	0.019
A_51_P481592	CKAP2	−1.98	1.00E-04	0.046
A_51_P450033	CDK1	−1.98	7.90E-05	0.044
A_51_P455897	FAM64A	−1.99	1.00E-04	0.047
A_51_P191649	NDC80	−2.03	8.30E-05	0.044
A_52_P559748	Hist1h2bq	−2.07	8.20E-05	0.044
A_52_P411003	DLGAP5	−2.07	5.30E-06	0.019
A_52_P1060609	AK087779	−2.08	1.00E-07	0.004
A_52_P415229	POLQ	−2.10	1.20E-05	0.025
A_51_P294346	MIS18BP1	−2.10	7.90E-05	0.044
A_52_P392544	CDCA8	−2.15	5.40E-05	0.043
A_51_P490509	BUB1B	−2.16	6.90E-05	0.043
A_52_P556462	FANCD2	−2.21	1.10E-05	0.024
A_51_P326769	Gnas	−2.23	8.60E-05	0.045
A_51_P127412	KIF15	−2.26	6.40E-05	0.043
A_52_P227880	CENPF	−2.28	1.10E-04	0.047

[a]Included are all genes altered by at least 1.5-fold in expression and detected with a FDR of less than 0.05.

Nadadur *et al.*, 2005; Williams *et al.*, 2007). In the present study, using the dataset of 55 genes differentially expressed at 24 h post-O_3 exposure with an FDR set at 5%, it was mainly cell cycle-associated functions including cell division/proliferation that were altered after acute O_3 exposure in the developing neonatal lung. This is illustrated by a large set of functional genes

that were significantly down-regulated by 24 h after acute O_3 exposure in the newborn lung. It is noteworthy that most of the genes down-regulated at 6 h post O_3 are also associated with cell cycle function, suggesting that this negative impact of O_3 on cell division/proliferation may have been initiated early but did not reach statistical significance at 5% FDR until 24 h post exposure. The decreased expression of cell cycle function genes suggested a decrease in cell division/proliferation. Analysis of BrdU incorporation further demonstrated that this suppression of the cell cycle was associated with reduced cell proliferation in the lung of O_3-exposed neonatal mice.

TABLE 3
Top List of Functional Groups Enriched by Genes Differentially Expressed in Newborn Lung at 24 h After O_3 Exposure[a]

Functional Group	Enrichment Score	No. of Genes in Group
Cellular process	12.14*	27
Cell cycle	39.84*	18
Cell division	20.91*	10
Cell cycle process	16.03*	9
Microtubule-based process	5.48*	3
Cell proliferation	4.29*	3
Transmembrane transport	1.06	1
Cellular metabolic process	1.03	10
Cell communication	0.81	1
Response to stimulus	3.73*	9
Cellular response to stimulus	10.13*	7
Response to stress	8.07*	6
Response to abiotic stimulus	1.25	1
Response to chemical stimulus	1.08	2
Cellular component organization	3.14*	6
Organelle organization	5.46*	5
Macromolecular complex assembly	0.72	1

[a]GO enrichment was performed through Partek Genomic Suite Software.
* Enrichment p-value < .05

The postnatal period is characterized by rapid growth and alveolarization of the developing lung. Differences exist between rodents and human in lung development stages. In human, alveolarization begins shortly before birth, whereas in mice it begins postnatally within two days after birth (Pinkerton and Joad, 2000). Nonetheless, in both cases, the postnatal lungs are developing rapidly and cell division/proliferation is a major component of this postnatal development phase. Therefore, it is conceivable that similar adverse effects of O_3 exposure on cell proliferation may also occur in the developing postnatal human lung. Alveolarization is a complex process coordinated by multiple interactions involving paracrine mechanisms between fibroblasts, epithelial cells, extracellular matrix, and vascular compartments of the lung. In the present study, none of the growth/differentiation factors, transcription factors or extracellular matrix components, previously shown to play a critical role in alveologenesis (Bourbon *et al.*, 2005; Maeda *et al.*, 2007; Mariani *et al.*, 2002) was significantly altered at 6 or 24 h after acute O_3 exposure. This suggests that alveolarization may not be affected at least in the short term by acute O_3 exposure. However, altered proliferation consistent with decreased expression of cyclin and Cdk in type-II alveolar epithelial cells has been associated with altered alveolar development in the premature baboon model of bronchopulmonary dysplasia (Das and Ravi, 2004). Whether altered alveolar cell proliferation may persist in the developing postnatal lung leading to altered alveolar development after chronic O_3 exposure needs to be determined.

Studies from this laboratory (Gabehart *et al.*, 2011) and others (Johnston et al., 2000a, 2006; Vancza *et al.*, 2009) clearly indicate that the magnitude of the lung response to O_3 exposure

TABLE 4
Top Networks of Genes Differentially Expressed in Newborn Lung at 24 h After O_3 Exposure

Functions	Molecules in Network	Score	Focus Molecules
Cell cycle, cellular assembly and organization, DNA replication, recombination, and repair	APC (complex), **BRCA1**, **BUB1B**, **CCNE1**, **CCNF**, CD3, **CDC45**, **CDCA2**, **CDK1**, **CENPF**, **CKAP2**, Cyclin A, **DBF4**, **DLGAP5**, E2f, **FANCD2**, **FANCI**, Histone H1, Histone h3, Histone h4, **KIF15**, **MELK**, **MKI67**, **MTHFD2**, **NCAPD2**, **NCAPH**, **NDC80**, NFkB (complex), Rb, RNA polymerase II, **RRM2**, **STIL**, **TACC3**, **UHRF1**, Vegf	55	24
Cell cycle, cellular assembly and organization, DNA replication, recombination, and repair	**ANKLE1**, ARNT, BYSL, **CCDC99**, CDA, **CENPK**, **CENPN**, **CHADL**, **CKAP2L**, **DCK**, DDX19B, **DEPDC1B**, **ESCO2**, GK, GOLM1, GPS2, **KIAA1524**, KNTC1, MAPRE3, **MIS18BP1**, NUP155, **PARPBP**, PPME1, PPP2R5D, **RAD54L**, RANBP1, SAE1, SPAG5, **TMEM48**, TRO, **TROAP**, UBA2, UBC, ZW10, ZWILCH	30	15

Network analyses were generated through the use of Ingenuity Systems software. Focus molecules are highlighted with bold character.

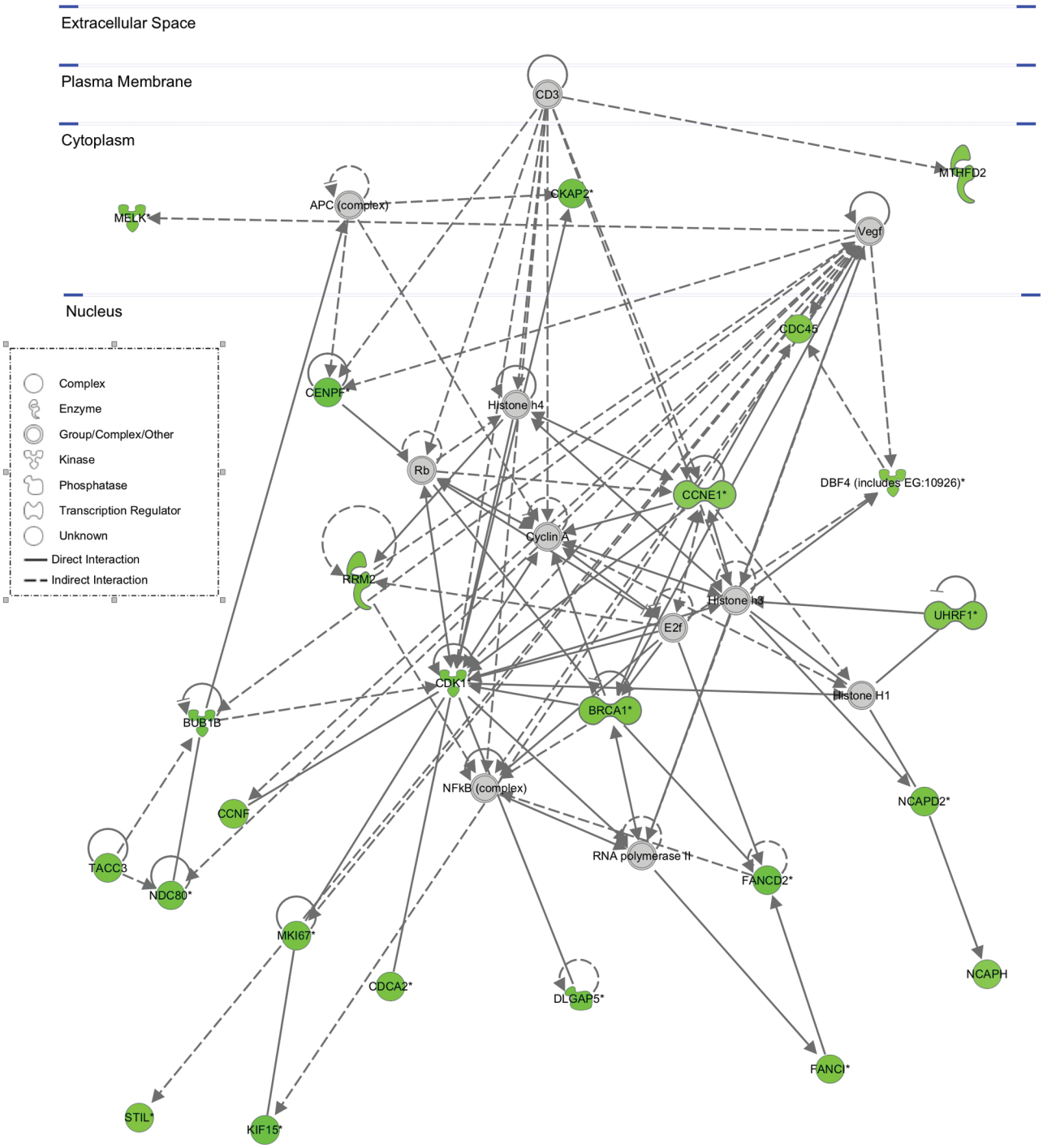

FIG. 5. Top ranked network of genes altered in the newborn lung at 24 h post-O_3 exposure. The gene network was generated with Ingenuity Pathway Analysis software using dataset of genes significantly altered by at least 1.5-fold (FDR, $q < .05$). This network had the highest enrichment score of 55 and contained 24 identified genes, all down-regulated by 24 h after O_3 exposure. The network is a graphical representation of knowledge-based functional relationships between molecules. Molecules are represented as nodes, and the biological relationship between two nodes is represented as a line. All relationships are supported by at least one reference from the literature stored in the Ingenuity Knowledge Base.

is much smaller in the early age than in adults. Therefore, it is possible that some of the O_3 response genes may not be detected on the microarrays due to low expression levels below the sensitivity of detection by this method. Using rt-qPCR to confirm the microarray data, we found that some of the genes (eg, CDK1, BRCA, RORC) were significantly altered at 6 h

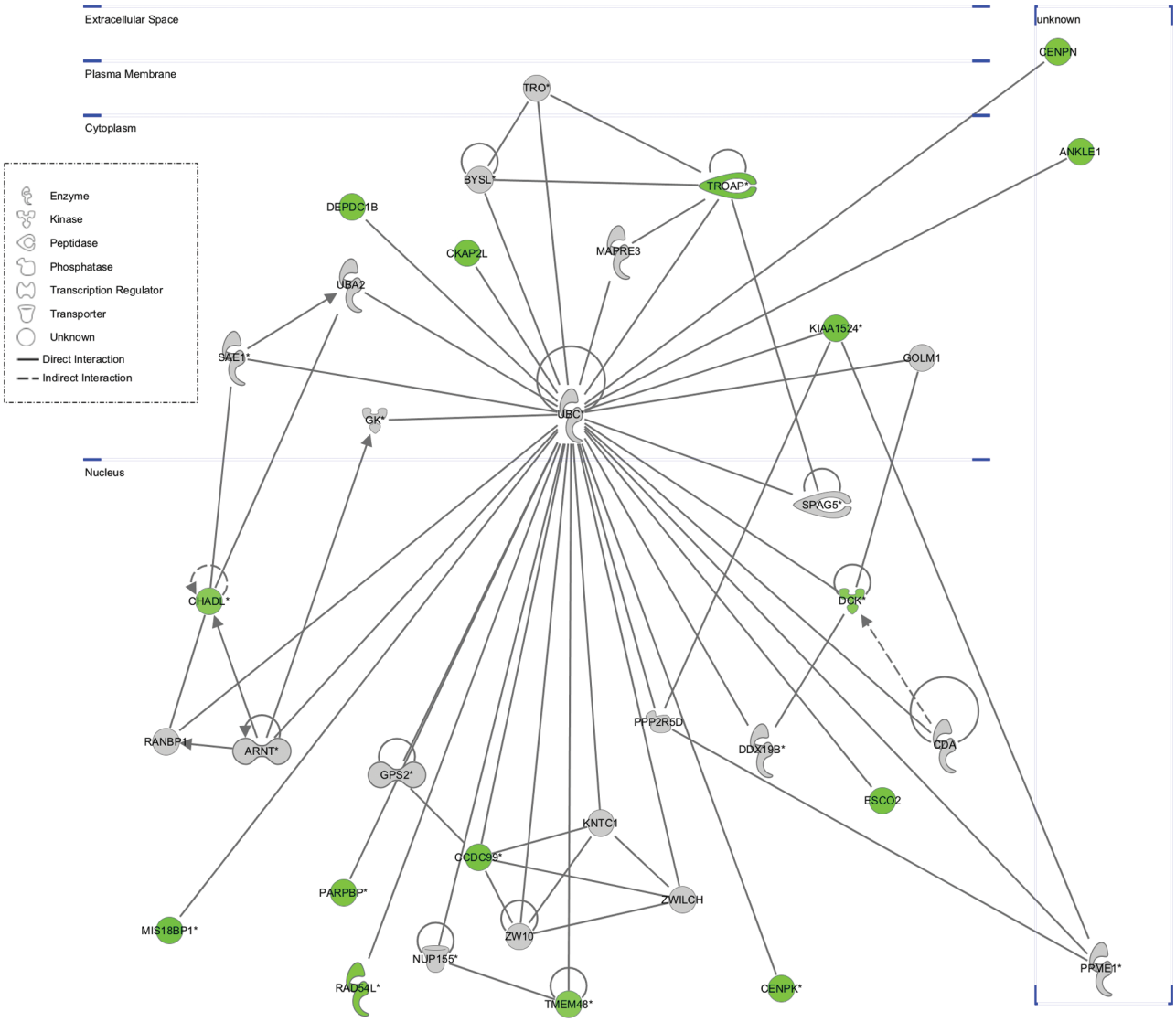

FIG. 6. Second ranked network of genes altered in the newborn lung at 24 h post-O_3 exposure. The gene network was generated with Ingenuity Pathway Analysis software using dataset of genes significantly altered by at least 1.5-fold (FDR, $q < .05$). This network has a score of 30 and contained 15 focus genes, all down-regulated by 24 h after O_3 exposure.

after O_3 exposure (Fig. 7), even though they were eliminated in the microarray analysis based on the Benjamini–Hochberg multiple comparison tests. Similarly, other genes (eg, CXCL-1, Hmox-1, MT-1) known to be induced after acute O_3 exposure (Johnston *et al.*, 2000b; Takahashi *et al.*, 1997; Valacchi *et al.*, 2004) were also up-regulated in the newborn lung as detected by rt-qPCR (Fig. 1) but were filtered out in the microarray analysis based on a FDR cutoff value of 5%.

O_3 is highly reactive but poorly soluble in water; hence it damages lung tissue indirectly by reacting with unsaturated fatty acids and other components in the epithelial lining fluid to create reactive oxygen radicals (Kennedy *et al.*, 1992; Pryor, 1992; Pryor and Church, 1991). Our microarray data indicate that O_3 induced OSGIN1 and GPX2 expression at 6 h in the newborn mouse lung (Table 1). OSGIN1 (also called OKL38) is an oxidative stress response gene stimulated by oxidized phospholipids that may regulate the differentiation and proliferation of cells through regulation of cell death (Li *et al.*, 2007). GPX2 is a selenium-dependent glutathione peroxidase that could play a role against toxicity of hydroperoxides and mediated inflammation (Esworthy *et al.*, 2005). The antioxidants MT-1 and Hmox-1 were also induced in our newborn mouse model of O_3 exposure (Fig. 1). MT-1 scavenges hydroxyl radicals to protect DNA from oxidative damage (Chubatsu and Meneghini, 1993), and acts as a zinc donor for DNA-repair enzymes (Sato and Bremmer, 1993). MT-1 could play a protective role against O_3-mediated lung inflammation via the regulation of pulmonary epithelial barrier and its anti-oxidative property (Inoue *et al.*, 2008). In the present study, albumin levels were not increased significantly in the BAL fluid of newborn mice following acute O_3 exposure and no

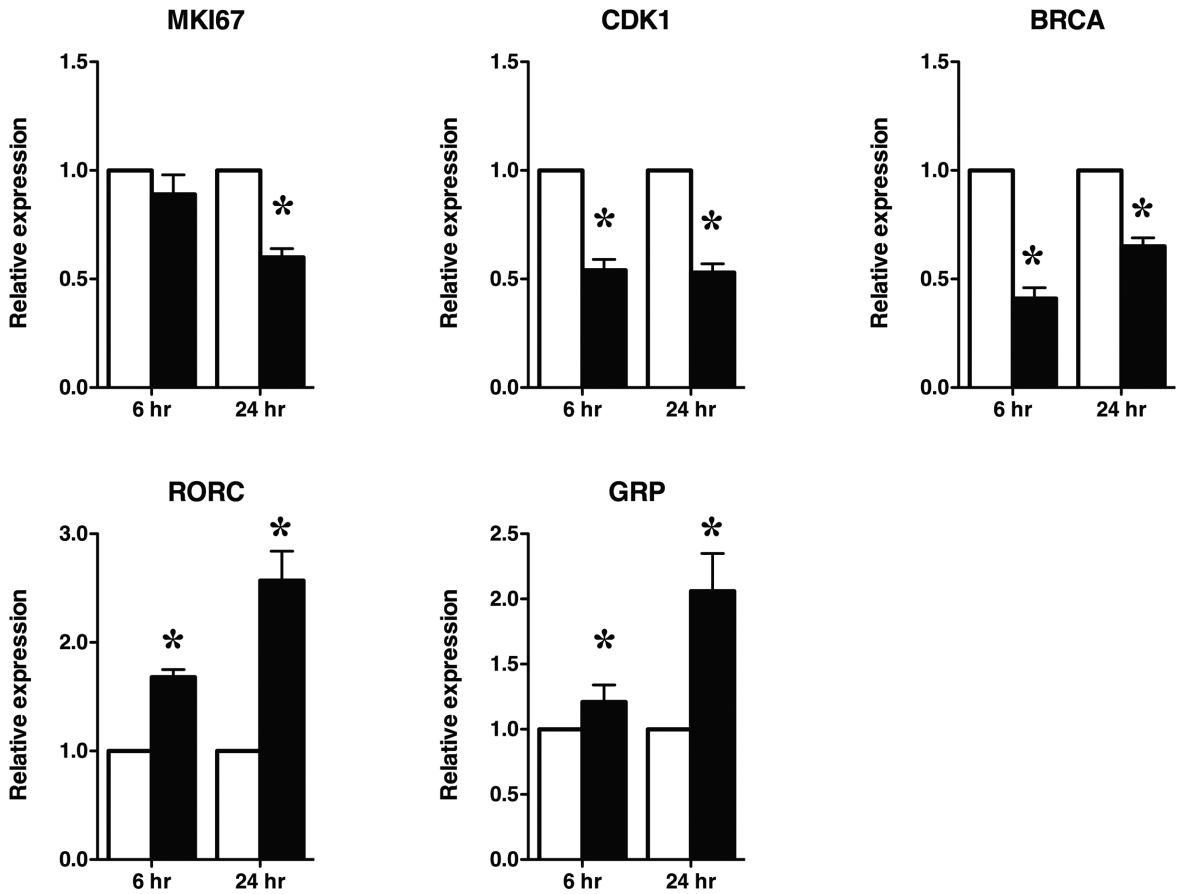

FIG. 7. Validation of differential expression for selected genes by RT-qPCR. Changes in gene expression were validated by RT-qPCR, confirming the results of microarrays for the same selected genes (MKI67, CDK1, BRCA, RORC, GRP). *Significant statistical difference ($p < .01$), when compared to FA.

obvious alteration in airway tissue or epithelial cell detachment could be detected under light microscopy. However, examination by electron microscopy showed clear alterations in the epithelial structure with enlarged intercellular space and disrupted junctions between adjacent cells in the tracheas of O_3 exposed newborn mice. This is in contrast to previous studies in adult rats where epithelial damage tended to occur more in distal airways than in the proximal airways after 8 h of exposure to 1000 ppb O_3 (Oslund *et al.*, 2009). This apparent difference may be due to differences in the age of animals and duration of O_3 exposure.

The first week of postnatal development is also a critical window of immune development in mice, in human this window extends to 1 year after birth (Dietert *et al.*, 2000), and an inappropriate response during this window may result in the development of aberrant responses on subsequent re-exposures. Previous studies have shown that infection of neonatal mice with respiratory syncytial virus during the first week of life predisposes to the development of an asthma-like phenotype characterized by a Th2 response and eosinophilc inflammation on subsequent re-infection at an older age, an aberrant response that did not develop in mice initially infected as weanling adults (Dakhama *et al.*, 2005). Subsequent studies further demonstrated that this aberrant response was due to a deficient interferon-γ production characterizing the immature response of newborn mice to RSV (Lee *et al.*, 2008). A recent study, using an infant rhesus monkey model, suggested that the immaturity of the immune system also could be a factor that determined the development of eosinophilic airway inflammation after repeated O_3 exposures (Maniar-Hew *et al.*, 2011). In the present study, no significant eosinophilic response was detected in the neonatal mouse lung after acute O_3 exposure; however, this may be due to the single exposure nature of our model. Future studies of chronic exposure during postnatal development in the neonatal mouse model may be necessary to further characterize this response and define underlying mechanisms.

At this early age, the innate immune system still generally favors a Th17 type response and a curtailed Th1 type response (Corbett *et al.*, 2010). The development of Th17 is critically dependent on the transcription factor retinoid-related orphan receptor (ROR)γt (Ivanov *et al.*, 2006). Our data showing increased expression of RORC, the gene encoding for RORγt, suggests that O_3 exposure may promote the development of Th17 cells in the neonatal mouse lung. Additionally, the gene transcript for pre-B lymphocyte 3 (VPREB3) was also increased in the neonatal lung after O_3 exposure, suggesting potential B cell involvement in the neonatal response to O_3.

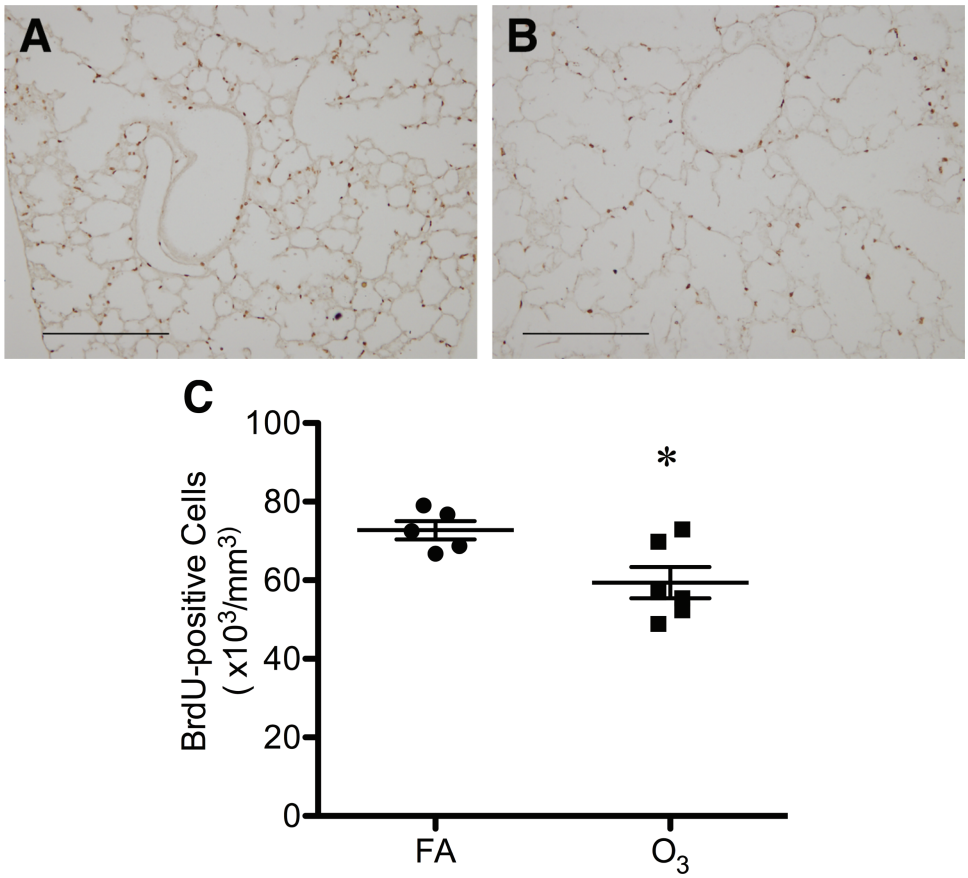

FIG. 8. Effect of acute O_3 exposure on cellular proliferation in the newborn lung. Lung tissues were collected at euthanasia, 24 h after exposure to FA (A) or O_3 (B). BrdU was administered by injection 3 h before euthanasia and was detected in lung tissue sections by immunohistochemistry (dark nuclei). Number of proliferating (BrdU-labeled) cells were determined by quantitative stereology (C). *: Significant statistical difference ($p < .5$), when compared to FA.

Neutrophil recruitment to the lungs is a characteristic response to acute O_3 exposure in both human and animal models (Hollingsworth *et al.*, 2007; Mudway and Kelly, 2004), including newborn mice, as shown in the present study. Neonates have been shown to have an immature and attenuated neutrophil response to sepsis in both human and animal models (Melvan *et al.*, 2010). Our data demonstrate that neonates also develop an attenuated neutrophil response to O_3 exposure, most likely due to their immature innate immunity. Our rt-qPCR results demonstrate that this neutrophilic response is associated with increased expression of the neutrophilic chemokines CXCL-1 and CXCL-5 in the lungs of O_3-exposed newborn mice. Unlike in adult mice, CXCL-2 expression was not increased in the newborn lung after O_3 exposure in our study (data not shown). Ozone-mediated CXCL-1 expression has been reported previously in the lungs of juvenile mice (Johnston et al., 2000a, 2004), but not CXCL-5, which was increased earlier in response to O_3 exposure in the newborn mouse lung in the present study. This suggests that CXCL-5 might play an important role in early recruitment of neutrophils to the lung after O_3 exposure.

Neurogenic function may also play an important role in airway response to O_3 exposure. Acute inhalation of O_3 induced rapid shallow breathing and bronchoconstriction through afferent vagal C-fibers (Schelegle *et al.*, 1993; Taylor-Clark and Undem, 2010). Activation of sensory C fibers can lead to the release of CGRP and other neuropeptides in the airways. In our newborn mouse model, the results of rt-qPCR showed that CGRP mRNA expression was increased significantly (1.92 ± 0.16-fold) but transiently at 6 h post-O_3 exposure. CGRP may play a role in epithelial injury and repair after O_3 exposure as recently suggested (Oslund *et al.*, 2009). Our results also demonstrate increased expression of the neuropeptide GRP at 24 h post-O_3 exposure. GRP is expressed by neuro-epithelial cells and may play a role in lung alveolarization (Degan *et al.*, 2008; Subramaniam *et al.*, 2007).

Overall, the results of this study identify few similarities and major differences in the effects of O_3 exposure in the developing postnatal lung compared to fully developed lungs. As in fully developed lungs, O_3 inhalation triggers an antioxidant response and a neutrophilic airway inflammation in the developing postnatal lung, albeit of smaller magnitude. Of major significance in this study is the finding that O_3 mediated a global suppression of several genes involved in cell cycle and proliferation in the developing postnatal lung. Because cell proliferation is critical to lung tissue repair, development and growth, a deficit in cell

proliferation during postnatal lung development may potentially impact subsequent lung development, structure and function growth. There is evidence to suggest that chronic O_3 exposure during active lung development may lead to altered airway structure and lung function (Evans *et al.*, 2004; Fanucchi *et al.*, 2006; Gauderman *et al.*, 2002; Kajekar *et al.*, 2007). Chronic exposure to O_3 has also been associated with significant reduction in lung function growth in young children (Frischer *et al.*, 1999; Ihorst *et al.*, 2004; Rojas-Martinez *et al.*, 2007), perhaps due to some extent to altered cell proliferation and growth. A potential limitation in our study is that a single O_3 exposure does not mimic the chronic exposure in human. Nonetheless, our data provide an important insight into the early effects of O_3 exposure on the developing lung. Whether similar effects can be sustained during chronic exposure and lead to alteration in structure and function of the lung need to be further explored and defined.

SUPPLEMENTARY DATA

Supplementary data are available online at http://toxsci.oxfordjournals.org/.

FUNDING

This work was supported by the National Institutes of Health [P01 ES018181 and R01 HD053557 to A.D.].

ACKNOWLEDGMENTS

The authors thank Dr Daniel Laflamme (Center for Genes, Environment and Health, National Jewish Health) for performing RNA labeling and hybridization on microarrays and the Biological Resource Center personnel for assistance with animal handling and care.

REFERENCES

Akinbami, L. J., Lynch, C. D., Parker, J. D., and Woodruff, T. J. (2010). The association between childhood asthma prevalence and monitored air pollutants in metropolitan areas, United States, 2001–2004. *Environ. Res*. **110**(3), 294–301.

Babin, S. M., Burkom, H. S., Holtry, R. S., Tabernero, N. R., Stokes, L. D., Davies-Cole, J. O., DeHaan, K., and Lee, D. H. (2007). Pediatric patient asthma-related emergency department visits and admissions in Washington, DC, from 2001–2004, and associations with air quality, socio-economic status and age group. *Environ. Health* **6,** 9.

Benjamini, Y., and Hochberg, Y. (1995). Controling the false discovery rate: A practical and powerful approach to multipul testing. *J. Royal Stat. Soc. B* **57,** 289–300.

Bourbon, J., Boucherat, O., Chailley-Heu, B., and Delacourt, C. (2005). Control mechanisms of lung alveolar development and their disorders in bronchopulmonary dysplasia. *Pediatr. Res*. **57**(5), 38R–46R.

Chubatsu, L.S., and Meneghini R. (1993). Metallothionein protects DNA from oxidative damage. *Biochem. J*. **291,** 193–198.

Corbett, N. P., Blimkie, D., Ho, K. C., Cai, B., Sutherland, D. P., Kallos, A., Crabtree, J., Rein-Weston, A., Lavoie, P. M., Turvey, S. E., *et al*. (2010). Ontogeny of Toll-like receptor mediated cytokine responses of human blood mononuclear cells. *PLoS ONE* **5**(11), e15041.

Dakhama, A., Park, J. W., Taube, C., Joetham, A., Balhorn, A., Miyahara, N., Takeda, K., and Gelfand, E. W. (2005). The enhancement or prevention of airway hyperresponsiveness during reinfection with respiratory syncytial virus is critically dependent on the age at first infection and IL-13 production. *J. Immunol*. **175**(3), 1876–1883.

Das, K. C., and Ravi, D. (2004). Altered expression of cyclins and cdks in premature infant baboon model of bronchopulmonary dysplasia. *Antioxid. Redox Signal*. **6**:117–127.

Degan, S., Lopez, G. Y., Kevill, K., and Sunday, M. E. (2008). Gastrin-releasing peptide, immune responses, and lung disease. *Ann. N. Y. Acad. Sci*. **1144,** 136–147.

Dietert, R. R., Etzel, R. A., Chen, D., Halonen, M., Holladay, S. D., Jarabek, A. M., Landreth, K., Peden, D. B., Pinkerton, K., Smialowicz, R. J., *et al*. (2000). Workshop to identify critical windows of exposure for children's health: Immune and respiratory systems work group summary. *Environ. Health Perspect*. **108**(Suppl. 3), 483–490.

Esworthy, R. S., Yang, L., Frankel, P. H., and Chu, F. F. (2005). Epithelium-specific glutathione peroxidase, Gpx2, is involved in the prevention of intestinal inflammation in selenium-deficient mice. *J. Nutr*. **135**(4), 740–745.

Evans, M. J., Fanucchi, M. V., Baker, G. L., Van Winkle, L. S., Pantle, L. M., Nishio, S. J., Schelegle, E. S., Gershwin, L. J., Miller, L. A., Hyde, D. M., *et al*. (2004). The remodelled tracheal basement membrane zone of infant rhesus monkeys after 6 months of recovery. *Clin. Exp. Allergy* **34**(7), 1131–1136.

Fanucchi, M. V., Plopper, C. G., Evans, M. J., Hyde, D. M., Van Winkle, L. S., Gershwin, L. J., and Schelegle, E. S. (2006). Cyclic exposure to ozone alters distal airway development in infant rhesus monkeys. *Am. J. Physiol. Lung Cell. Mol. Physiol*. **291**(4), L644–L650.

Finkelstein, J. N., and Johnston, C. J. (2004). Enhanced sensitivity of the postnatal lung to environmental insults and oxidant stress. *Pediatrics* **113**(4 Suppl.), 1092–1096.

Frischer, T., Studnicka, M., Gartner, C., Tauber, E., Horak, F., Veiter, A., Spengler, J., Kuhr, J., and Urbanek, R. (1999). Lung function growth and ambient ozone: A three-year population study in school children. *Am. J. Respir. Crit. Care Med*. **160**(2), 390–396.

Gabehart, K., Correll, K. A., Yang, J., Collins, M. L., Loader, J. E., White, C. W., and Dakhama, A. (2011). Effect of postnatal ozone exposure on the developing lung. *Am. J. Respir. Crit. Care Med.* **183**, A3242.

Gauderman, W. J., Gilliland, G. F., Vora, H., Avol, E., Stram, D., McConnell, R., Thomas, D., Lurmann, F., Margolis, H. G., Rappaport, E. B., *et al*. (2002). Association between air pollution and lung function growth in southern California children: Results from a second cohort. *Am. J. Respir. Crit. Care Med*. **166**(1), 76–84.

Gohil, K., Cross, C. E., and Last, J. A. (2003). Ozone-induced disruptions of lung transcriptomes. *Biochem. Biophys. Res. Commun*. **305**(3), 719–728.

Hicks, A., Kourteva, G., Hilton, H., Li, H., Lin, T. A., Liao, W., Li, Y., Wei, X., March, T., Benson, J., *et al*. (2010). Cellular and molecular characterization of ozone-induced pulmonary inflammation in the Cynomolgus monkey. *Inflammation* **33**(3), 144–156.

Holladay, S. D., and Smialowicz, R. J. (2000). Development of the murine and human immune system: Differential effects of immunotoxicants depend on time of exposure. *Environ. Health Perspect*. **108**(Suppl. 3), 463–473.

Hollingsworth, J. W., Kleeberger, S. R., and Foster, W. M. (2007). Ozone and pulmonary innate immunity. *Proc. Am. Thorac. Soc*. **4**(3), 240–246.

Ihorst, G., Frischer, T., Horak, F., Schumacher, M., Kopp, M., Forster, J., Mattes, J., and Kuehr, J. (2004). Long- and medium-term ozone effects on lung growth including a broad spectrum of exposure. *Eur. Respir. J*. **23**(2), 292–299.

Inoue, K., Takano, H., Kaewamatawong, T., Shimada, A., Suzuki, J., Yanagisawa, R., Tasaka, S., Ishizaka, A., and Satoh, M. (2008). Role of metallothionein in lung inflammation induced by ozone exposure in mice. *Free Radic. Biol. Med*. **45**(12), 1714–1722.

Ivanov, II, McKenzie, B. S., Zhou, L., Tadokoro, C. E., Lepelley, A., Lafaille, J. J., Cua, D. J., and Littman, D. R. (2006). The orphan nuclear receptor RORgammat directs the differentiation program of proinflammatory IL-17+ T helper cells. *Cell* **126**(6), 1121–1133.

Johnston, C. J., Oberdorster, G., Gelein, R., and Finkelstein, J. N. (2000a). Newborn mice differ from adult mice in chemokine and cytokine expression to ozone, but not to endotoxin. *Inhal. Toxicol*. **12**(3), 205–224.

Johnston, C. J., Reed, C. K., Avissar, N. E., Gelein, R., and Finkelstein, J. N. (2000b). Antioxidant and inflammatory response after acute nitrogen dioxide and ozone exposures in C57Bl/6 mice. *Inhal. Toxicol*. **12**(3), 187–203.

Johnston, C. J., Holm, B. A., and Finkelstein, J. N. (2004). Differential proinflammatory cytokine responses of the lung to ozone and lipopolysaccharide exposure during postnatal development. *Exp. Lung Res*. **30**(7), 599–614.

Johnston, C. J., Holm, B. A., Gelein, R., and Finkelstein, J. N. (2006). Postnatal lung development: Immediate-early gene responses post ozone and LPS exposure. *Inhal. Toxicol*. **18**(11), 875–883.

Kajekar, R., Pieczarka, E. M., Smiley-Jewell, S. M., Schelegle, E. S., Fanucchi, M. V., and Plopper, C. G. (2007). Early postnatal exposure to allergen and ozone leads to hyperinnervation of the pulmonary epithelium. *Respir. Physiol. Neurobiol*. **155**(1), 55–63.

Kennedy, C. H., Hatch, G. E., Slade, R., and Mason, R. P. (1992). Application of the EPR spin-trapping technique to the detection of radicals produced in vivo during inhalation exposure of rats to ozone. *Toxicol. Appl. Pharmacol*. **114**(1), 41–46.

Knust, J., Ochs, M., Gundersen, H. J., and Nyengaard, J. R. (2009). Stereological estimates of alveolar number and size and capillary length and surface area in mice lungs. *Anat. Rec. (Hoboken)* **292**(1), 113–122.

Lee, Y. M., Miyahara, N., Takeda, K., Prpich, J., Oh, A., Balhorn, A., Joatham, A., Gelfand, E. W., and Dakhama, A. (2008). IFN-gamma production during initial infection determines the outcome of reinfection with respiratory syncytial virus. *Am. J. Respir. Crit. Care Med*. **177**(2), 208–218.

Li, R., Chen, W., Yanes, R., Lee, S., and Berliner, J. A. (2007). OKL38 is an oxidative stress response gene stimulated by oxidized phospholipids. *J. Lipid Res*. **48**(3), 709–715.

Maeda, Y., Davé, V., and Whitsett, J. A. (2007). Transcriptional control of lung morphogenesis. *Physiol. Rev*. **87,** 219–244.

Maniar-Hew, K., Postlethwait, E. M., Fanucchi, M. V., Ballinger, C. A., Evans, M. J., Harkema, J. R., Carey, S. A., McDonald, R. J., Bartolucci, A. A., and Miller, L. A. (2011). Postnatal episodic ozone results in persistent attenuation of pulmonary and peripheral blood responses to LPS challenge. *Am. J. Physiol. Lung Cell. Mol. Physiol*. **300**(3), L462–L471.

Mar, T. F., and Koenig, J. Q. (2009). Relationship between visits to emergency departments for asthma and ozone exposure in greater Seattle, Washington. *Ann. Allergy Asthma Immunol*. **103**(6), 474–479.

Mariani, T. J., Reed, J. J., and Shapiro, S. D. (2002). Expression profiling of the developing mouse lung. Insights into the establishment of the extracellular matrix. *Am. J. Respir. Cell. Mol. Biol*. **26,** 541–548.

Melvan, J. N., Bagby, G. J., Welsh, D. A., Nelson, S., and Zhang, P. (2010). Neonatal sepsis and neutrophil insufficiencies. *Int. Rev. Immunol*. **29**(3), 315–348.

Mudway, I. S., and Kelly, F. J. (2004). An investigation of inhaled ozone dose and the magnitude of airway inflammation in healthy adults. *Am. J. Respir. Crit. Care Med*. **169**(10), 1089–1095.

Nadadur, S. S., Costa, D. L., Slade, R., Silbjoris, R., and Hatch, G. E. (2005). Acute ozone-induced differential gene expression profiles in rat lung. *Environ. Health Perspect*. **113**(12), 1717–1722.

Oslund, K. L., Hyde, D. M., Putney, L. F., Alfaro, M. F., Walby, W. F., Tyler, N. K., and Schelegle, E. S. (2009). Activation of calcitonin gene-related peptide receptor during ozone inhalation contributes to airway epithelial injury and repair. *Toxicol. Pathol*. **37**(6), 805–813.

Park, J. W., Taube, C., Joetham, A., Takeda, K., Kodama, T., Dakhama, A., McConville, G., Allen, C. B., Sfyroera, G., Shultz, L. D., *et al*. (2004). Complement activation is critical to airway hyperresponsiveness after acute ozone exposure. *Am. J. Respir. Crit. Care Med*. **169**(6), 726–732.

Pinkerton, K. E., and Joad, J. P. (2000). The mammalian respiratory system and critical windows of exposure for children's health. *Environ. Health Perspect*. **108**(Suppl. 3), 457–462.

Plopper, C. G., and Fanucchi, M. V. (2000). Do urban environmental pollutants exacerbate childhood lung diseases? *Environ. Health Perspect*. **108**(6), A252–A253.

Pryor, W. A., and Church, D. F. (1991). Aldehydes, hydrogen peroxide, and organic radicals as mediators of ozone toxicity. *Free Radic. Biol. Med*. **11**(1), 41–46.

Pryor, W. A. (1992). How far does ozone penetrate into the pulmonary air/tissue boundary before it reacts? *Free Radic. Biol. Med*. **12**(1), 83–88.

Rojas-Martinez, R., Perez-Padilla, R., Olaiz-Fernandez, G., Mendoza-Alvarado, L., Moreno-Macias, H., Fortoul, T., McDonnell, W., Loomis, D., and Romieu, I. (2007). Lung function growth in children with long-term exposure to air pollutants in Mexico City. *Am. J. Respir. Crit. Care Med*. **176**(4), 377–384.

Romieu, I., Sienra-Monge, J. J., Ramirez-Aguilar, M., Tellez-Rojo, M. M., Moreno-Macias, H., Reyes-Ruiz, N. I., del Rio-Navarro, B. E., Ruiz-Navarro, M. X., Hatch, G., Slade, R., *et al*. (2002). Antioxidant supplementation and lung functions among children with asthma exposed to high levels of air pollutants. *Am. J. Respir. Crit. Care Med*. **166**(5), 703–709.

Roy, M. G., Rahmani, M., Hernandez, J. R., Alexander, S. N., Ehre, C., Ho, S. B., and Evans, C. M. (2011). Mucin production during prenatal and postnatal murine lung development. *Am. J. Respir. Cell Mol. Biol*. **44**(6), 755–760.

Sato, M., and Bremmer, I. (1993). Oxygen free radicals and metallothionein. *Free Radic. Biol. Med*. **14,** 325–337.

Schelegle, E. S., Carl, M. L., Coleridge, H. M., Coleridge, J. C., and Green, J. F. (1993). Contribution of vagal afferents to respiratory reflexes evoked by acute inhalation of ozone in dogs. *J. Appl. Physiol*. **74**(5), 2338–2344.

Strickland, M. J., Darrow, L. A., Klein, M., Flanders, W. D., Sarnat, J. A., Waller, L. A., Sarnat, S. E., Mulholland, J. A., and Tolbert, P. E. (2010). Short-term associations between ambient air pollutants and pediatric asthma emergency department visits. *Am. J. Respir. Crit. Care Med*. **182**(3), 307–316.

Strickland, M. J., Darrow, L. A., Mulholland, J. A., Klein, M., Flanders, W. D., Winquist, A., and Tolbert, P. E. (2011). Implications of different approaches for characterizing ambient air pollutant concentrations within the urban airshed for time-series studies and health benefits analyses. *Environ. Health* **10,** 36.

Subramaniam, M., Bausch, C., Twomey, A., Andreeva, S., Yoder, B. A., Chang, L., Crapo, J. D., Pierce, R. A., Cuttitta, F., and Sunday, M. E. (2007). Bombesin-like peptides modulate alveolarization and angiogenesis in bronchopulmonary dysplasia. *Am. J. Respir. Crit. Care Med*. **176**(9), 902–912.

Tager, I. B., Balmes, J., Lurmann, F., Ngo, L., Alcorn, S., and Kunzli, N. (2005). Chronic exposure to ambient ozone and lung function in young adults. *Epidemiology* **16**(6), 751–759.

Takahashi, Y., Takahashi, S., Yoshimi, T., Miura, T., Mochitate, K., and Kobayashi, T. (1997). Increases in the mRNA levels of gamma-glutamyltransferase and heme oxygenase-1 in the rat lung after ozone exposure. *Biochem. Pharmacol*. **53**(7), 1061–1064.

Taylor-Clark, T. E., and Undem, B. J. (2010). Ozone activates airway nerves via the selective stimulation of TRPA1 ion channels. *J. Physiol*. **588**(Pt 3), 423–433.

Triche, E. W., Gent, J. F., Holford, T. R., Belanger, K., Bracken, M. B., Beckett, W. S., Naeher, L., McSharry, J. E., and Leaderer, B. P. (2006). Low-level

ozone exposure and respiratory symptoms in infants. *Environ. Health Perspect*. **114**(6), 911–916.

Valacchi, G., Pagnin, E., Corbacho, A. M., Olano, E., Davis, P. A., Packer, L., and Cross, C. E. (2004). In vivo ozone exposure induces antioxidant/stress-related responses in murine lung and skin. *Free Radic. Biol. Med*. **36**(5), 673–681.

Vancza, E. M., Galdanes, K., Gunnison, A., Hatch, G., and Gordon, T. (2009). Age, strain, and gender as factors for increased sensitivity of the mouse lung to inhaled ozone. *Toxicol. Sci*. **107**(2), 535–543.

White, M. C., Etzel, R. A., Wilcox, W. D., and Lloyd, C. (1994). Exacerbations of childhood asthma and ozone pollution in Atlanta. *Environ. Res*. **65**(1), 56–68.

Williams, A. S., Issa, R., Leung, S. Y., Nath, P., Ferguson, G. D., Bennett, B. L., Adcock, I. M., and Chung, K. F. (2007). Attenuation of ozone-induced airway inflammation and hyper-responsiveness by c-Jun NH2 terminal kinase inhibitor SP600125. *J. Pharmacol. Exp. Ther*. **322**(1), 351–359.